



Modeling the impact of heterogeneous reactions of chlorine on summertime nitrate formation in Beijing, China

Xionghui Qiu^{1,2}, Qi Ying³, Shuxiao Wang^{1,2}, Lei Duan^{1,2}, Jian Zhao⁴, Jia Xing^{1,2}, Dian Ding^{1,2}, Yele Sun⁴, Baoxian Liu⁵, Aijun Shi⁶, Xiao Yan⁶, Qingcheng Xu^{1,2}, and Jiming Hao^{1,2}

¹State Key Joint Laboratory of Environmental Simulation and Pollution Control, School of Environment, Tsinghua University, Beijing 100084, China

²State Environmental Protection Key Laboratory of Sources and Control of Air Pollution Complex, School of Environment, Tsinghua University, Beijing 100084, China

³Zachry Department of Civil Engineering, Texas A&M University, College Station, Texas 77843-3138, USA

⁴State Key Laboratory of Atmospheric Boundary Layer Physics and Atmospheric Chemistry, Institute of Atmospheric Physics, Chinese Academy of Sciences, Beijing 100029, China

⁵Beijing Environmental Monitoring Center, Beijing 100048, China

⁶Beijing Municipal Research Institute of Environmental Protection, Beijing 100037, China

Correspondence: Qi Ying (qying@civil.tamu.edu) and Shuxiao Wang (shxwang@tsinghua.edu.cn)

Received: 6 December 2018 – Discussion started: 20 December 2018

Revised: 9 May 2019 – Accepted: 10 May 2019 – Published: 21 May 2019

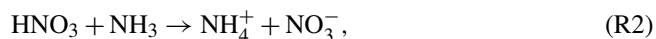
Abstract. Comprehensive chlorine heterogeneous chemistry is incorporated into the Community Multiscale Air Quality (CMAQ) model to evaluate the impact of chlorine-related heterogeneous reaction on diurnal and nocturnal nitrate formation and quantify the nitrate formation from gas-to-particle partitioning of HNO_3 and from different heterogeneous pathways. The results show that these heterogeneous reactions increase the atmospheric Cl_2 and ClNO_2 level ($\sim 100\%$), which further affects the nitrate formation. Sensitivity analyses of uptake coefficients show that the empirical uptake coefficient for the O_3 heterogeneous reaction with chlorinated particles may lead to the large uncertainties in the predicted Cl_2 and nitrate concentrations. The N_2O_5 uptake coefficient with particulate Cl^- concentration dependence performs better in capturing the concentration of ClNO_2 and nocturnal nitrate concentration. The reaction of OH and NO_2 in the daytime increases the nitrate by $\sim 15\%$ when the heterogeneous chlorine chemistry is incorporated, resulting in more nitrate formation from HNO_3 gas-to-particle partitioning. By contrast, the contribution of the heterogeneous reaction of N_2O_5 to nitrate concentrations decreases by about 27% in the nighttime, when its reactions with chlorinated particles are considered. However, the generated gas-phase ClNO_2 from the heterogeneous reaction of

N_2O_5 and chlorine-containing particles further reacts with the particle surface to increase the nitrate by 6%. In general, this study highlights the potential of significant underestimation of daytime concentrations and overestimation of nighttime nitrate concentrations for chemical transport models without proper chlorine chemistry in the gas and particle phases.

1 Introduction

In recent years, nitrate has become the primary component of $\text{PM}_{2.5}$ (particulate matter with an aerodynamic diameter less than $2.5\ \mu\text{m}$) in Beijing, with sustained and rapid reduction of SO_2 and primary particulate matter emissions (Ma et al., 2018; Li et al., 2018; Wen et al., 2018). Observations showed that the relative contributions of secondary nitrate in $\text{PM}_{2.5}$ could reach up to approximately 50% during some severe haze pollution days (Li et al., 2018). The mechanism of secondary nitrate formation can be summarized as two major pathways. (1) Gas-to-particle partitioning of HNO_3 happens mostly in the daytime. The reaction of OH with NO_2 produces gaseous HNO_3 , which subsequently partitions into the particle phase. The existence of NH_3 or basic parti-

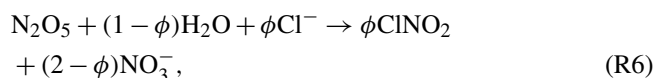
cles enhances this process by $\text{NH}_3\text{-NH}_4^+$ gas–particle equilibrium (Kleeman et al., 2005; Seinfeld and Pandis, 2006). (2) Hydrolysis of N_2O_5 is more important during the nighttime, when N_2O_5 forms from the reactions of NO_2 , O_3 and NO_3 and hydrolyzes to produce particulate nitrate. They can be summarized as Reactions (R1)–(R5) (Brown and Stutz, 2012):



In addition to Reactions (R1) and (R5), gas-phase reactions of NO_3 with HO_2 and VOCs, N_2O_5 with water vapor (Tuaizon et al., 1983), and the heterogeneous reaction of NO_2 with the water-containing particle (Goodman et al., 1999) produce HNO_3 or nitrate as well. These reactions are listed in Table 2 as Reactions (R8), (R9) and (R10).

However, chemistry transport models (CTMs) incorporated with these mechanisms still cannot accurately capture the spatiotemporal distributions of nitrate in some studies in polluted northern China. For example, Chang et al. (2018) showed that the simulated nitrate concentrations derived from the default Community Multiscale Air Quality (CMAQ; version 5.0.2) were significantly higher than the observations in summer at two sites adjacent to Beijing. Fu et al. (2016) also found that the default CMAQ (version 5.0.1) overestimated the simulated nitrate concentrations in the Beijing–Tianjin–Hebei region.

In recent field studies, it was found that high particulate chlorine emissions might have a significant impact on the oxidation capacity of the urban atmosphere and thus could affect nitrate concentrations. According to the field measurements in June 2017 in Beijing (Zhou et al., 2018), the 2 min averaged concentrations of reactive molecular chlorine (Cl_2) and nitryl chloride (ClNO_2) reached up to 1000 and 1200 pptv, respectively, during some severe air pollution periods in summer. The Cl_2 concentrations were significantly higher than those observed in North American coastal cities affected by onshore flow and the lower atmosphere in the remote Arctic region (Spicer et al., 1998; Glasow, 2010; Liu et al., 2017). During these pollution events, the corresponding concentrations of N_2O_5 (2 min average) and nitrate (5 min average) rose from 40 pptv and $1 \mu\text{g m}^{-3}$ to 700 pptv and $5 \mu\text{g m}^{-3}$. To explain the high levels of ClNO_2 , some studies suggested that Reaction (R5) should be revised to account for ClNO_2 production from the heterogeneous reaction of N_2O_5 on chloride-containing particles (CPs; Osthoff et al., 2008; Thornton et al., 2010), as shown in Reaction (R6):



where ϕ represents the molar yield of ClNO_2 . By incorporating this reaction into WRF-Chem, Li et al. (2016) found that the improved model performed better in matching the observed nitrate concentrations in Hong Kong during 15 November and 5 December 2013. However, ClNO_2 could affect the formation of nitrate indirectly by increasing the atmospheric OH after a series of chemical reactions, which are briefly summarized into three steps: (1) the photolysis of ClNO_2 produces chlorine radicals (Cl^\bullet), (2) the reaction of Cl^\bullet with VOCs produces the peroxy radical (HO_2 and RO_2), and (3) the increased HO_2 and RO_2 prompt the formation of OH through the HO_x cycle and lead to increased HNO_3 production (Young et al., 2014; Jobson et al., 1994). The overall impact of Reaction (R6) on nitrate remains to be investigated.

Another related but unresolved issue is the sources of the high concentrations of Cl_2 , which could not be explained by the N_2O_5 heterogeneous reaction with Cl^- and the subsequent reactions of ClNO_2 in the gas phase. It has been reported that the reactions of gaseous O_3 , OH, HO_2 , ClNO_2 , hypochlorous acid (HOCl) and chlorine nitrate (ClONO_2) with CPs can produce Cl_2 , which can subsequently photolyze to produce Cl^\bullet (Knipping et al., 2000; George and Abbatt, 2010; Pratte and Rossi, 2006; Deiber et al., 2004; Faxon et al., 2015). However, these heterogeneous reactions in CPs are generally missing in most of the current CTMs, and it is unclear whether these reactions will be able to explain the observed Cl_2 concentrations and the overall impact of these reactions on nitrate.

Previously, biomass burning, coal combustion and waste incineration were identified as the main sources of gaseous and particulate chlorine compounds in China from the International Global Atmospheric Chemistry program's Global Emissions Inventory Activity (GEIA) based on the year 1990 and a localized study by Fu et al. (2018) based on the year 2014 (Keene et al., 1999; Fu et al., 2018). However, recent source apportionment results of $\text{PM}_{2.5}$ in Beijing showed that the contribution of coal combustion had extremely decreased from 22.4 % in 2014 to 3 % in 2017 with the replacement of natural gas (obtained from official website of the Beijing Municipal Bureau of Statistics, available at <http://edu.bjstats.gov.cn/>, last access: 5 May 2018). Another important source – cooking – has received attention with its increasing contribution to $\text{PM}_{2.5}$ (accounting for 33 % of the residential sector; obtained from the official source apportionment analysis of $\text{PM}_{2.5}$ in Beijing in 2017; see <http://sthjj.beijing.gov.cn/>, last access: 5 May 2018). Moreover, the high content of particulate sodium chloride was measured from the source characterization studies of $\text{PM}_{2.5}$ released from the cooking activities (Zhang et al., 2016). Thus, it is necessary to compile an updated emission inventory for Beijing to include the emissions from cooking and other sources (coal burning, solid waste incineration, biomass burning, etc.) in order to explore the emissions of the chlorine species on atmospheric nitrate formation.

In this study, a CMAQ model with improved chlorine heterogeneous chemistry is applied to simulate summer nitrate concentration in Beijing. Sensitivity simulations are conducted to evaluate the contributions of HNO₃ gas-to-particle partitioning and heterogenous production to aerosol nitrate. The results of this work can improve our understandings on nitrate formation and provide useful information on nitrate pollution control strategies in Beijing.

2 Emissions, chemical reactions and model description

2.1 Emissions

Generally, the conventional emission inventories of air pollutants in China only include the common chemical species, such as SO₂, NO_x, VOCs, PM_{2.5}, PM₁₀, NH₃, BC and OC (Wang et al., 2014). Chloride compound emissions were not included. However, the emissions of chlorine species are vital for studying the chlorine chemical mechanism. Recently, the inorganic hydrogen chloride (HCl) and fine particulate chloride (PCL) emission inventories for the sectors of coal combustion, biomass burning and waste incineration were developed for the year 2014 (Qiu et al., 2016; Fu et al., 2018; Liu et al., 2018). However, gaseous chlorine emissions were not estimated in these studies. In addition, these studies did not account for the rapid decrease in coal consumption in recent years in Beijing, from 2000 Mt in 2014 to 490 Mt in 2017. More importantly, the cooking source, as one of the major contributors to particulate chlorine in Beijing, is not included in current chlorine emission inventories. Thus, a new emission inventory of reactive chlorine species, which includes HCl, Cl₂ and PCL, was developed in this study for the year 2017.

The emission factor method (Eq. 1) is applied to calculate the emissions of these reactive chlorine species from coal combustion, biomass burning, municipal solid waste incineration and industrial processes:

$$E_{i,j} = A_i \times EF_{i,j}, \quad (1)$$

where $E_{i,j}$ represents the emission factor of pollutant j in sector i , A represents the activity data and EF represents the emission factor. The EF for PCL is estimated by $EF_{i,PCL} = EF_{i,PM_{2.5}} \times f_{Cl,i}$, where $f_{Cl,i}$ represents the mass fraction of PCL in primary PM_{2.5}. Activity data are obtained from the Beijing Municipal Bureau of Statistics (available at <http://tjj.beijing.gov.cn/>, last access: 4 May 2018). The Cl₂ emission factor for coal combustion is calculated based on the content of Cl in coal, which was measured by Deng et al. (2014). The PM_{2.5} emission factors and mass fractions of PCL in PM_{2.5} to calculate the emissions of Cl were described in detail by Fu et al. (2018). PCL in PM_{2.5} for coal combustion and biomass burning is taken as 1 % and 9.0 %, respectively, based on local measurements in Beijing.

Table 1. The sectoral emissions of HCl, Cl₂ and PCL in Beijing in 2017 (unit: Mg yr⁻¹).

Sector	Emissions		
	HCl	Cl ₂	PCL
Power plant	22.8	1.2	6.75
Industry	587.3	20.1	89.2
Residential	202.4	8.1	34.7
Biomass burning	0.182	0	0.14
Municipal solid waste	1080.2	0	8.47
Cooking	0	0	426.8
Total	1892.9	29.4	566.1

Emissions of PCL from cooking, including contributions from commercial and household cooking, are estimated using Eq. (2):

$$E_{PCL} = [N_f \times V_f \times H_f \times EF_{f,PCL} + V_c \times H_c \times N_c \times n \times EF_{c,PCL} \times (1 - \eta)] \times 365, \quad (2)$$

where N_f is the number of households; V_f is the volume of exhaust gas from a household stove (2000 m³ h⁻¹); H_f is the cooking time for a family (0.5 h d⁻¹); $EF_{f,PCL}$ and $EF_{c,PCL}$ are the emission factors (kg m⁻³) of PCL for household and commercial cooking, respectively; H_c is the cooking time in a commercial cooking facility (6 h d⁻¹); N_c is the number of restaurants, schools and government departments; V_c is the volume of exhaust gas from a commercial cooking stove (8000 m³ h⁻¹); and n is the number of stoves for each unit, which is six for a restaurant and is calculated as one stove per 150 students for each school. η is the removal efficiency of fume scrubbers (30 %). $EF_{c,PCL}$ is the emission factor (kg m⁻³) of PCL in commercial cooking. These constants are all based on Wu et al. (2018). The PCL fraction in PM_{2.5} from cooking is taken as 10 %, based on local measurements. HCl and Cl₂ emissions from cooking are not considered in this study.

The sectoral emissions of HCl, Cl₂ and PCL are summarized in Table 1. The estimated HCl, Cl₂ and PCL emissions in Beijing are 1.89, 0.07 and 0.63 Gg, respectively. The Cl emissions estimated for 2014 by Fu et al. (2018) were used for other areas. This simplification is a good approximation because replacing coal with natural gas only occurred in Beijing, and reduction of coal consumption in surrounding regions was generally less than 15 %. In addition, strict control measures for biomass burning, cooking and municipal solid waste incineration have not been implemented in most regions yet. Emissions of conventional species for this study period are developed in a separate study that is currently under review and are summarized in Table S1 in the Supplement.

Table 2. Major gas-phase and heterogeneous pathway of producing nitrate in original CMAQ, and newly added or revised heterogeneous reactions in improved CMAQ.

Type	Reactions	no.	Reference	Comment
Original CMAQ				
Gas-phase chemistry	$\text{OH} + \text{NO}_2 \rightarrow \text{HNO}_3$	R1		
	$\text{N}_2\text{O}_5 + \text{H}_2\text{O} \rightarrow 2\text{HNO}_3$	R7		
	$\text{HO}_2^* + \text{NO}_3 \rightarrow 0.2\text{HNO}_3 + 0.8\text{OH}^* + 0.8\text{NO}_2$	R8		
	$\text{NO}_3 + \text{VOCs}^* \rightarrow \text{HNO}_3$	R9		
Heterogeneous chemistry	$\text{N}_2\text{O}_5(\text{g}) + \text{H}_2\text{O}(\text{aq}) \rightarrow 2\text{H}^+ + 2\text{NO}_3^-$	R5		
	$2\text{NO}_2(\text{g}) + \text{H}_2\text{O}(\text{aq}) \rightarrow \text{HONO}(\text{g}) + \text{H}^+ + \text{NO}_3^-$	R10		
Improved CMAQ				
Newly added or revised heterogeneous reactions	$\text{N}_2\text{O}_5(\text{g}) + \text{H}_2\text{O}(\text{aq}) + \text{Cl}^-(\text{aq}) \rightarrow \text{ClONO}_2(\text{g}) + \text{NO}_3^-$	R6	Bertram and Thornton (2009)	Revise R5
	$2\text{NO}_2(\text{g}) + \text{Cl}^- \rightarrow \text{ClNO}(\text{g}) + \text{NO}_3^-$	R11	Abbatt and Waschewsky (1998)	Revise R10
	$\text{NO}_3(\text{g}) + 2\text{Cl}^- \rightarrow \text{Cl}_2(\text{g}) + \text{NO}_3^-$	R12	Rudich et al. (1996)	Increase NO_3^-
	$\text{O}_3(\text{g}) + 2\text{Cl}^- + \text{H}_2\text{O}(\text{aq}) \rightarrow \text{Cl}_2(\text{g}) + \text{O}_2(\text{g}) + 2\text{OH}^-$	R13	Abbatt and Waschewsky (1998)	Affect OH
	$2\text{OH}^*(\text{g}) + 2\text{Cl}^- \rightarrow \text{Cl}_2(\text{g}) + 2\text{OH}^-$	R14	George and Abbatt (2010)	Affect OH
	$\text{ClONO}_2(\text{g}) + \text{Cl}^- \rightarrow \text{Cl}_2(\text{g}) + \text{NO}_3^-$	R15	Deiber et al. (2004)	Affect OH
	$\text{HOCl}(\text{g}) + \text{Cl}^- + \text{H}^+ \rightarrow \text{Cl}_2(\text{g}) + \text{H}_2\text{O}$	R16	Pratte and Rossi (2006)	Affect OH
	$\text{ClONO}_2(\text{g}) + \text{Cl}^- + \text{H}^+ \rightarrow \text{Cl}_2(\text{g}) + \text{HONO}(\text{g})$ (pH < 2.0)	R17	Riedel et al. (2012)	Affect OH
	$\text{ClONO}_2(\text{g}) + \text{H}_2\text{O}(\text{aq}) \rightarrow \text{Cl}^- + \text{NO}_3^- + 2\text{H}^+$ (pH ≥ 2.0)	R18	Rossi (2003)	Increase NO_3^-

* Different VOC species. In the SAPRC-11 mechanism, the VOC species include CCHO (acetaldehyde), RCHO (lumped C3+ aldehydes), GLY (glyoxal), MGLY (methylglyoxal), PHEN (phenols), BALD (aromatic aldehydes), MACR (methacrolein) and IPRD (lumped isoprene product species).

2.2 Chlorine-related heterogeneous reactions

The heterogeneous reactions in original CMAQ (version 5.0.1) are not related to chlorine species. In this study, the original heterogeneous reactions of N_2O_5 and NO_2 (Reactions R5 and R10 in Table 2) are replaced with a revised version which includes production of ClONO_2 from CPs (Reactions R6 and R11 in Table 2). In Reaction (R6), the molar yield of ClONO_2 (ϕ_{ClONO_2}) is represented as Eq. (3) (Bertram and Thornton, 2009):

$$\phi_{\text{ClONO}_2} = \left(1 + \frac{[\text{H}_2\text{O}]}{483 \times [\text{Cl}^-]}\right)^{-1}, \quad (3)$$

where $[\text{H}_2\text{O}]$ and $[\text{Cl}^-]$ are the molarities of liquid water and chloride (mol m^{-3}), respectively.

In addition, laboratory observations confirmed that the heterogeneous uptake of some oxidants (such as O_3 and OH) and reactive chlorine species (such as ClONO_2 , HOCl and ClONO_2) could also occur in CPs to produce Cl_2 . These reactions are implemented in the model and summarized in Table 2 as Reactions (R13)–(R18). Note that the products from the heterogeneous uptake of ClONO_2 in CPs vary with particle acidity (Riedel et al., 2012; Rossi, 2003). It generates Cl_2 under the condition of the pH being lower than 2 but produces nitrate and chloride under higher pH conditions. The reaction rates of the heterogeneous reactions are parameterized as first-order reactions, with the rate of change of gas-phase species concentrations determined by Eq. (4) (Ying et

al., 2015):

$$\frac{dC}{dt} = -\frac{1}{4}(v\gamma A)C = -k^I C, \quad (4)$$

where C represents the concentration of species, v represents the thermal velocity of the gas molecules (m s^{-1}), A is the CMAQ-predicted wet aerosol surface area concentration ($\text{m}^2 \text{m}^{-3}$) and γ represents the uptake coefficient. For all gas phases, for species (except ClONO_2) involved in the heterogeneous reactions (Reactions R6 and R11–R18), a simple analytical solution can be used to update their concentrations from time t_0 to $t_0 + \Delta t$: $[C]_{t_0+\Delta t} = [C]_{t_0} \exp(-k^I \Delta t)$, where Δt is the operator-splitting time step for heterogeneous reactions.

The rate of change of ClONO_2 includes both removal and production terms, as shown in Eq. (5):

$$\begin{aligned} \frac{d[\text{ClONO}_2]}{dt} &= -k_i^I [\text{ClONO}_2] + k_6^I \phi_{\text{ClONO}_2} [\text{N}_2\text{O}_5] \\ &= -k_i^I [\text{ClONO}_2] + k_6^I \phi_{\text{ClONO}_2} [\text{N}_2\text{O}_5]_{t_0} \exp(-k_6^I t). \end{aligned} \quad (5)$$

Assuming that ϕ_{ClONO_2} is a constant, an analytical solution for Eq. (5) can be obtained, as shown in Eq. (6):

$$\begin{aligned} [\text{ClONO}_2]_{t_0+\Delta t} &= [\text{ClONO}_2]_{t_0} \exp(-k_i^I \Delta t) \\ &+ \frac{k_6^I \phi_{\text{ClONO}_2} [\text{N}_2\text{O}_5]_{t_0}}{k_i^I - k_6^I} [\exp(-k_6^I \Delta t) - \exp(-k_i^I \Delta t)], \end{aligned} \quad (6)$$

where k_i^I represents the pseudo-first-order rate coefficient of either Reaction (R17) or (R18), depending on pH.

The uptake coefficients γ of gaseous species are obtained from published laboratorial studies. In the original CMAQ, the uptake coefficient of N_2O_5 is determined as a function of the concentrations of $(\text{NH}_4)_2\text{SO}_4$, NH_4HSO_4 and NH_4NO_3 (Davis et al., 2008). In this study, the parameterization dependent on $\text{P}(\text{Cl})$ and NO_3^- by Bertram and Thornton (2009) (Eq. 7) is used:

$$\gamma_{\text{N}_2\text{O}_5} = \begin{cases} 0.02, & \text{for frozen aerosols} \\ 3.2 \times 10^{-8} K_f \left[1 - \left(1 + \frac{6 \times 10^{-2} [\text{H}_2\text{O}]}{[\text{NO}_3^-]} + \frac{29 [\text{Cl}]}{[\text{NO}_3^-]} \right)^{-1} \right], & \end{cases} \quad (7)$$

In the above equation, K_f is parameterized function based on the molarity of water: $K_f = 1.15 \times 10^6 (1 - e^{-0.13 [\text{H}_2\text{O}]})$. NO_3^- and Cl^- concentrations are also molar. The uptake coefficient of OH is expressed in Eq. (8) as a function of the concentration of $\text{P}(\text{Cl})$ following the IUPAC (International Union of Pure and Applied Chemistry, available at http://iupac.poleether.fr/htdocs/datasheets/pdf/O-H-halide_solutions_VI.A2.1.pdf, last access: 5 June 2018).

$$\gamma_{\text{OH}} = \min \left(0.04 \times \frac{[\text{Cl}^-]}{1000 \times M}, 1 \right), \quad (8)$$

where M represents the volume of liquid water in aerosol volume ($\text{m}^3 \text{m}^{-3}$). For frozen particles, the uptake coefficient is limited to 0.02, as used in the original CMAQ model.

The uptake coefficients of O_3 , NO_3 , NO_2 , HOCl , ClONO_2 and ClONO_2 are treated as constants. Among of them, the γ values of NO_3 , NO_2 , HOCl and ClONO_2 are set as 3×10^{-3} , 1×10^{-4} , 1.09×10^{-3} and 0.16 based on laboratory measurements (Rudich et al., 1996; Abbatt and Waschewsky, 1998; Pratte and Rossi, 2006; Gebel and Finlayson-Pitts, 2001). A preliminary value of 10^{-3} in the daytime and 10^{-5} during the nighttime is chosen for the O_3 uptake coefficient. The daytime γ_{O_3} is based on the analysis of the Cl_2 production rate in a hypothesized geochemical cycle of reactive inorganic chlorine in the marine boundary layer by Keene et al. (1990). The lower nighttime value was also recommended by Keene et al. (1990), who noted that Cl_2 production in the marine boundary layer is lower at night. The uptake coefficient of ClONO_2 depends on the particle acidity, with the value of 2.65×10^{-6} for Reaction (R17) and 6×10^{-3} for Reaction (R18) (Roberts et al., 2008).

2.3 CMAQ model configuration

These heterogeneous reactions of chlorine are incorporated into a revised CMAQ based on the CMAQ version 5.0.1 to simulate the distribution of nitrate concentration in Beijing from 11 to 15 June 2017. The revised CMAQ model without heterogeneous reactions of chlorine has been described in detail by Ying et al. (2015) and Hu et al. (2016, 2017). In summary, the gas-phase chemical mechanism in the revised

CMAQ model is based on the SAPRC-11 (Carter and Heo, 2013) with comprehensive inorganic chlorine chemistry. Reactions of the Cl radical with several major VOCs, which lead to production of HCl , are also included. The aerosol module is based on AERO6, with an updated treatment of the NO_2 and SO_2 heterogeneous reaction and formation of secondary organic aerosol from isoprene epoxides. Three-level nested domains with the resolutions of 36, 12 and 4 km using Lambert conformal conic projection (173×136 , 135×228 and 60×66 grid cells) are chosen in this work (the domains; see Fig. S1). The two true latitudes are set to 25 and 40° N, and the origin of the domain is set at 34° N, 110° E. The left-bottom coordinates of the outmost domain are positioned at $x = -3114 \text{ km}$, $y = -2448 \text{ km}$. The BASE case (heterogeneous reactions of Cl turned off) and HET case (all heterogeneous reactions enabled) are compared to evaluate the impact of heterogeneous chlorine chemistry on nitrate formation.

3 Results

3.1 Model performance evaluation

Predicted O_3 , NO_2 and $\text{PM}_{2.5}$ concentrations from the BASE case simulation are evaluated against monitoring data at 12 sites in Beijing (Table S2) in 11 to 15 June 2017. The average values for normalized mean bias (NMB) for O_3 , NO_2 and $\text{PM}_{2.5}$ across the 12 sites are -8% , -7% and -8% , respectively, and 29%, 59% and 53% for normalized mean error (NME), respectively. Predicted hourly Cl_2 , ClONO_2 and N_2O_5 concentrations were compared with observations measured at the Institute of Atmospheric Physics (IAP), Chinese Academy of Sciences (39.98° N, 116.37° E), using a high-resolution time-of-flight chemical ionization mass spectrometer (CIMS) from 11 to 15 June 2017 (for site description, instrument introduction and analytical method, please refer to the study by Zhou et al., 2018). Figure 1 shows that the concentrations of Cl_2 and ClONO_2 in the BASE case are rather low (close to 0), proving that the gas-phase chemistry is not the major pathway for producing Cl_2 and ClONO_2 . By contrast, the simulated Cl_2 and ClONO_2 concentrations in HET case increase significantly; correspondingly the NMB and NME changes from -100% to -54% and 100% to 61% for Cl_2 and from -100% to -58% and 100% to 62% for ClONO_2 , respectively (the particle surface area concentrations is scaled up by a factor of 5 during the daytime and 10 during the nighttime because this parameter is underestimated compared to the measured concentrations reported by Zhou et al., 2018). The simulations of Cl_2 and ClONO_2 are improved as the additional heterogeneous reactions prompt the production of gas-phase molecular chlorine. Overall, however, the Cl_2 and ClONO_2 concentrations are still underestimated. Both BASE and HET simulations generally capture the hourly N_2O_5 concentrations as well as the peak values (Fig. 1c) with similar overall NMB and NME values.

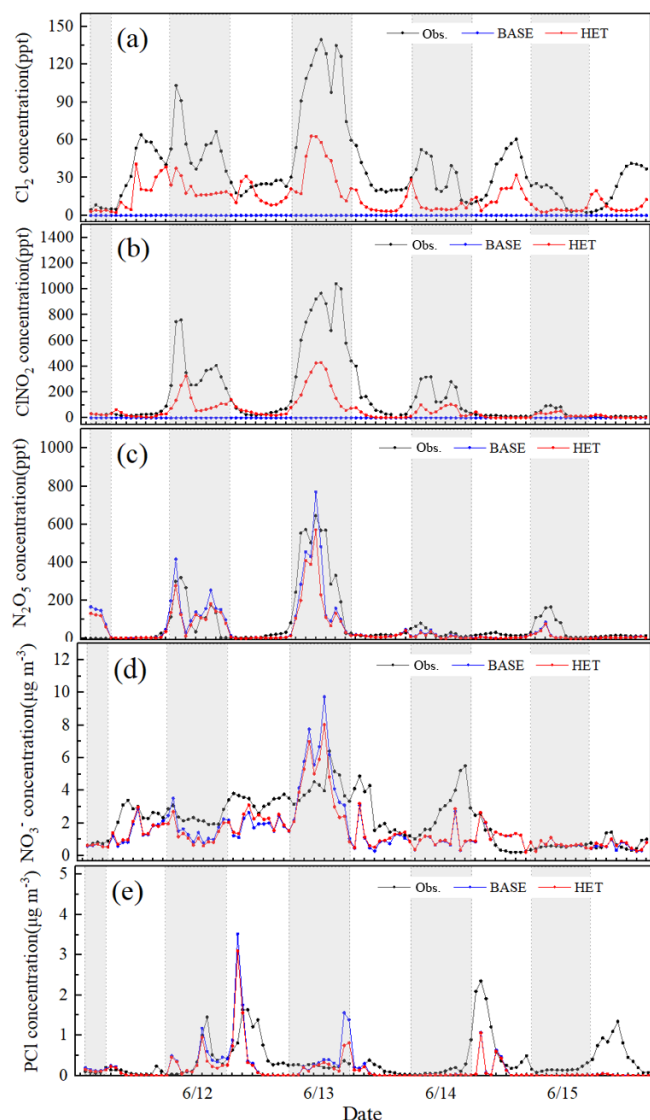


Figure 1. Comparison of observed hourly Cl_2 , ClNO_2 , N_2O_5 (at the Institute of Atmospheric Physics, Chinese Academy of Sciences), NO_3^- and PCl (at Tsinghua University) in urban Beijing with predictions from the BASE and the HET cases during 11–15 June 2017.

The uptake coefficient of O_3 could be an important factor affecting the predicted Cl_2 concentrations, as the heterogeneous reaction of O_3 is found to be the major source of Cl_2 during this period (see discussion in Sect. 3.2). The influence of different parametrizations of the uptake coefficient of N_2O_5 on ClNO_2 and nitrate concentrations are also discussed in Sect. 3.2.

Predicted NO_3^- and PCl concentrations are compared with observations measured at an adjacent monitoring site located at the rooftop of School of Environment building at Tsinghua University (THU; 40.00°N , 116.34°E ; about 5 km from the IAP) using an online analyzer of Monitoring for Aerosol and Gases in ambient Air (MARGA) from 11 to 15 June 2017.

According to Fig. 1d, the simulated nitrate concentration is slightly lower than the observations most of the time. From the evening hours of 12 June to the morning hours of 13 June, observed and simulated nitrate concentrations both increase significantly. The NMB and NME values of hourly nitrate for the HET case (-5% and 39% , respectively) are slightly lower than those for the BASE case (-10% and 46%) during this high-concentration period. The HET case also generally captures the day-to-day variation of PCl concentration and performs better than the BASE case, correspondingly the NMB and NME are reduced from -48% and 72% to -37% and 67% . The substantial underestimation of PCl in the daytime on 15 June is likely caused by missing local emissions during this period.

3.2 Impact of uptake coefficients of O_3 and N_2O_5 on chlorine species and nitrate

The uptake coefficients of O_3 and N_2O_5 may be important factors affecting the accuracy of simulated nitrate concentrations. Some studies have confirmed that the reaction of O_3 in CPs can indirectly affect the nitrate formation by increasing the atmospheric Cl_2 and OH level (Li et al., 2016; Liu et al., 2018). According to Fig. 1a, the improved model still substantially underestimates the concentration of Cl_2 , which may be associated with the underestimation of the uptake coefficients of O_3 , which are empirical and have not been confirmed by laboratory studies. The uptake coefficients were increased by a factor of 10 (0.01 for daytime and 10^{-4} for nighttime) to evaluate the sensitivity of Cl_2 production and nitrate formation to this parameter. Figure 2 shows that the simulated Cl_2 and nitrate concentrations in daytime increase significantly (especially for Cl_2) and can sometimes capture the peak value (such as the daytime peak on 14 June). However, although the NMB and NME of Cl_2 and nitrate improve from -18% and 39% to 1% and 28% when the new uptake coefficients are used, the simulated Cl_2 concentrations are still quite different from the observations (such as during the daytime on 11 and 12 June; see Fig. 2). A non-constant parameterization of the uptake coefficients of O_3 that considers the influence of PCl concentrations, meteorology conditions, etc., similar to those of OH and N_2O_5 , might be needed. Further laboratory studies should be conducted to provide a better estimation of this important parameter.

Several parameterizations for the uptake coefficient of N_2O_5 have been developed for regional and global models and have been evaluated in several previous studies (Tham et al., 2018; McDuffie et al., 2018a, b). In addition to the parameterization of Bertram and Thornton (2009) used in the HET case, two additional simulations were performed to assess the impact of the uptake coefficient of N_2O_5 on nitrate formation. The first simulation uses the original CMAQ parameterization of Davis et al. (2008), and the second simulation uses a constant value of 0.09 , which is the upper limit of the N_2O_5 uptake coefficient derived by Zhou et al. (2018),

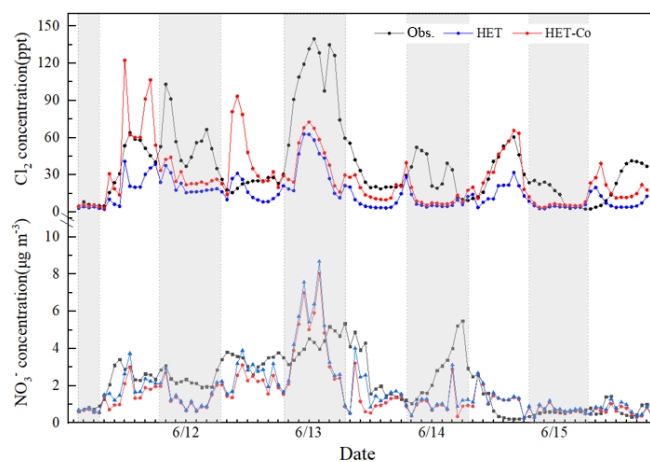


Figure 2. Comparison of observed and predicted Cl_2 and NO_3^- concentrations under different uptake coefficient of O_3 (HET: daytime is $\gamma_{\text{O}_3} = 1 \times 10^{-3}$, nighttime is $\gamma_{\text{O}_3} = 1 \times 10^{-5}$; HET-Co: daytime is $\gamma_{\text{O}_3} = 1 \times 10^{-2}$, nighttime is $\gamma_{\text{O}_3} = 1 \times 10^{-4}$).

based on observations. The results from the simulations with the parameterization of Bertram and Thornton (2009) generally agree with the results using those based on Davis et al. (2008). The application of a larger and fixed N_2O_5 uptake coefficient leads to slightly better results, which might reflect the fact that the N_2O_5 concentrations are underestimated. Using the uptake coefficient of 0.09 can generally increase the concentration of nitrate in some periods, but it also leads to significant increase in the nitrate level (such as nighttime on 12–13 June and 13–14 June), which is 4–6 times higher than those based on Bertram and Thornton (2009). Overall, predicted nitrate concentrations are sensitive to changes in $\gamma_{\text{N}_2\text{O}_5}$, with an increase of approximately 50% in the nitrate when a constant of $\gamma_{\text{N}_2\text{O}_5}$ of 0.09 is used.

3.3 Spatial distributions of nitrate and chlorine species concentrations

The regional distributions of averaged Cl_2 , ClNO_2 , N_2O_5 and NO_3^- concentration from 11 to 15 June for the HET case are shown in Fig. 3. Compared to the BASE case, the episode-average concentrations of Cl_2 and ClNO_2 from the HET case increase significantly in the eastern region of Beijing, reaching up to 23 and 71 ppt from near zero (Fig. 3a and b). High concentrations are not found in the southern region with intensive emissions of chlorine species (Fig. S2). The production of ClNO_2 requires the presence of chloride, NO_2 and O_3 . In the areas close to the fresh emissions, O_3 is generally low (Fig. S3), and the production of NO_3 (hence N_2O_5 and ClNO_2) is limited. Therefore, the production rate of ClNO_2 is generally low in areas affected by fresh emissions. Since the contribution of direct emissions to Cl_2 is low and it is predominantly produced secondarily in the atmosphere, high levels of Cl_2 are also found away from the fresh emissions.

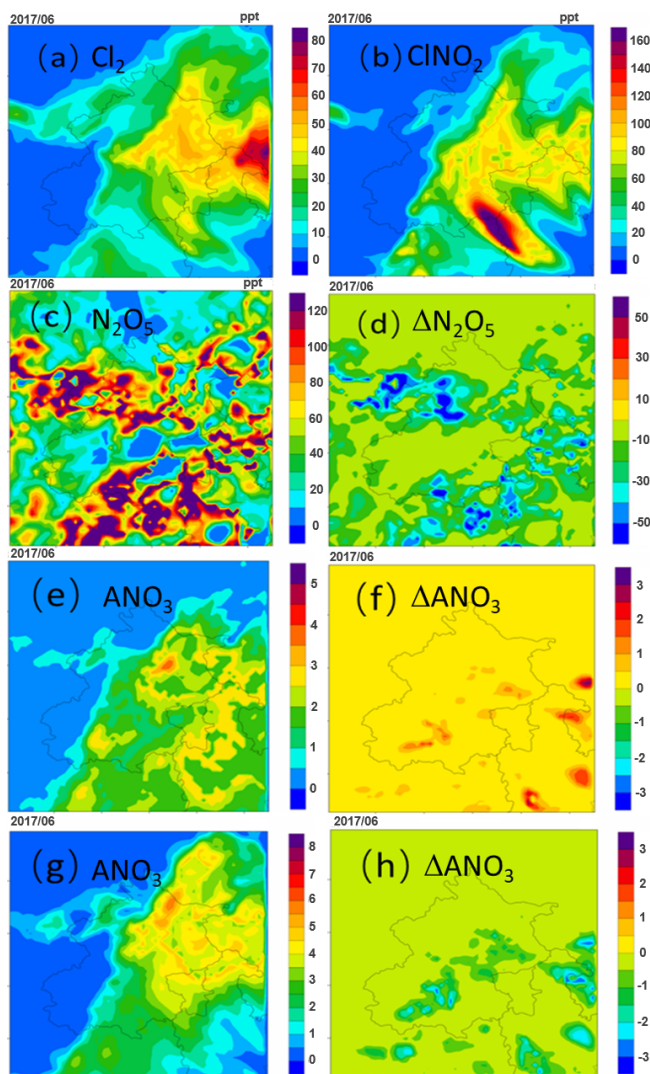


Figure 3. Spatial distributions of episode-average (a) Cl_2 , (b) ClNO_2 , (c) N_2O_5 , (e) daytime nitrate (ANO_3) and (g) nighttime nitrate concentrations from 11–15 June 2017, and the differences in the episode-average (d) N_2O_5 (HET case minus BASE case), (f) daytime nitrate and (g) nighttime nitrate (units are $\mu\text{g m}^{-3}$).

The spatial distribution of N_2O_5 concentrations differs from that of other species (Fig. 3c). While the concentrations of most of the species are higher in the southern region, the N_2O_5 concentrations are lower in some parts of this region. This is because the O_3 concentration in the core urban areas is low due to high NO_x emissions. The N_2O_5 concentrations from the HET case are approximately 16% lower on average (Fig. 3d) because the Bertram and Thornton (2009) parameterization used in the HET case generally gives higher uptake coefficients than the parameterization of Davis et al. (2008) used in the BASE case (Table 3).

Although the higher uptake coefficients of N_2O_5 in the HET case facilitate faster conversion of N_2O_5 to nitrate, the nitrate concentrations do not always increase. During day-

Table 3. Observed day (D) and night (N) NO_3^- concentrations (Obs.) and predicted uptake coefficient of N_2O_5 ($\gamma_{\text{N}_2\text{O}_5}$) and nitrate concentrations (Pred.) using the parameterizations of $\gamma_{\text{N}_2\text{O}_5}$ by Bertram and Thornton (2009; Scenario 1), Davis et al. (2008; Scenario 2) and the upper-limit value derived by Zhou et al. (2018; Scenario 3) from 11 to 15 June 2017.

	NO_3^- Obs.	Scenario 1		Scenario 2		Scenario 3	
		$\gamma_{\text{N}_2\text{O}_5}$	Pred.	$\gamma_{\text{N}_2\text{O}_5}$	Pred.	$\gamma_{\text{N}_2\text{O}_5}$	Pred.
06/11-D	2.54	0.033	1.59	0.008	1.32	0.09	2.17
06/11-12-N	2.42	0.043	1.67	0.037	1.37	0.09	2.12
06/12-D	3.39	0.028	2.16	0.032	2.74	0.09	3.13
06/12-13-N	4.24	0.021	4.02	0.022	4.05	0.09	6.04
06/13-D	2.57	0.012	1.18	0.008	1.06	0.09	2.47
06/13-14-N	4.10	0.022	4.45	0.022	4.45	0.09	7.13
06/14-D	0.95	0.001	1.34	0.001	1.33	0.09	1.64
06/14-15-N	2.75	0.013	1.00	0.007	0.96	0.09	2.33
06/15-D	0.75	0.001	0.66	0.001	0.66	0.09	1.11

time hours, nitrate concentrations in the HET case increase due to higher OH (Fig. 3e and f; for increased OH, see Fig. S4). During the nighttime, in contrast, the nitrate concentration decreases significantly in some regions by about 22 %, mainly due to lower molar yield of nitrate from the N_2O_5 heterogeneous reaction in the HET case (Fig. 3g and h). Although ClNO_2 produced in the N_2O_5 reaction also produces nitrate through a heterogeneous reaction when the particle pH is above 2, which is true for most regions (see Fig. S5), the uptake coefficient of ClNO_2 is significantly lower than that of N_2O_5 (0.01–0.09 for N_2O_5 and 6×10^{-3} for ClNO_2), leading to an overall decrease in nitrate production. As the ClNO_2 production from the heterogeneous reaction leads to less N_2O_5 conversion to non-relative nitrate, it may change the overall lifetime of NO_x and its transport distances. The magnitude of this change and its implications on ozone and $\text{PM}_{2.5}$ in local and downwind areas should be further studied.

3.4 Relationship between nitrate formation and chlorine chemistry

Nitrate production from the homogeneous and heterogeneous pathways in Beijing is approximated by the difference in predicted nitrate concentrations between the BASE or HET case and a sensitivity case without heterogeneous reactions. Averaging over the 5 d period, approximately 58 % of the nitrate originates from HNO_3 gas-to-particle partitioning and 42 % is from heterogeneous reactions (Fig. 4). This conclusion generally agrees with measurements at Peking University (PKU; 52 % from the heterogeneous process and 48 % from HNO_3 partitioning) on 4 polluted days (average in September 2016 reported by Wang et al., 2017). Slightly higher contributions of the homogeneous pathway in this study are expected because of high OH concentrations during the day and lower particle surface areas at night.

The nitrate formation from different homogeneous and heterogeneous pathways in the BASE case and HET case

are further studied. Contributions of different gas-phase pathways are determined using the process analysis tool in CMAQ. Contributions of different heterogeneous pathways are determined using a zero-out method that turns off one heterogeneous pathway at a time in a series of sensitivity simulations. Figure 4 shows that the reaction of OH and NO_2 is always the major pathway for the formation of nitrate through homogeneous formation of HNO_3 and gas-to-particle partitioning. However, its nitrate production rate through this homogeneous pathway decreases significantly from daytime to nighttime (from 1.81 to $0.33 \mu\text{g m}^{-3} \text{h}^{-1}$ on average). The nitrate production from other HNO_3 partitioning pathways in the daytime is negligible. During the nighttime, homogeneous reaction of N_2O_5 with water vapor accounts for approximately 5 % of the overall homogeneous nitrate formation. For the heterogeneous pathways, daytime production rate is approximately $0.6 \mu\text{g m}^{-3} \text{h}^{-1}$, with one-third of the contributions being from NO_2 and two-thirds from N_2O_5 . Nighttime production on nitrate from the heterogeneous pathways is approximately $3.1 \mu\text{g m}^{-3} \text{h}^{-1}$, of which 85 % is due to N_2O_5 and 15 % is due to NO_2 .

Comparing the BASE case and the HET case shows that, when the chlorine chemistry is included, the gaseous HNO_3 produced by OH reacting with NO_2 increases significantly in the HET case. Correspondingly, the nitrate production rate reaches up to $2.04 \mu\text{g m}^{-3} \text{h}^{-1}$ in the daytime due to increased atmospheric OH concentrations predicted by the chlorine reactions. Similar conclusions are also obtained by Li et al. (2016) and Liu et al. (2017) based on observations and model simulations. The heterogeneous production of nitrate from the reaction of N_2O_5 uptake decreases by approximately 27 % in the HET case due to the production of gas-phase ClNO_2 . According to the study by Sarwar et al. (2012, 2014), including the heterogeneous reaction of N_2O_5 with PCI decreased the nocturnal nitrate concentration by 11 %–21 % in the United States, which was slightly less than the current study for Beijing. It is likely because PCI concentra-

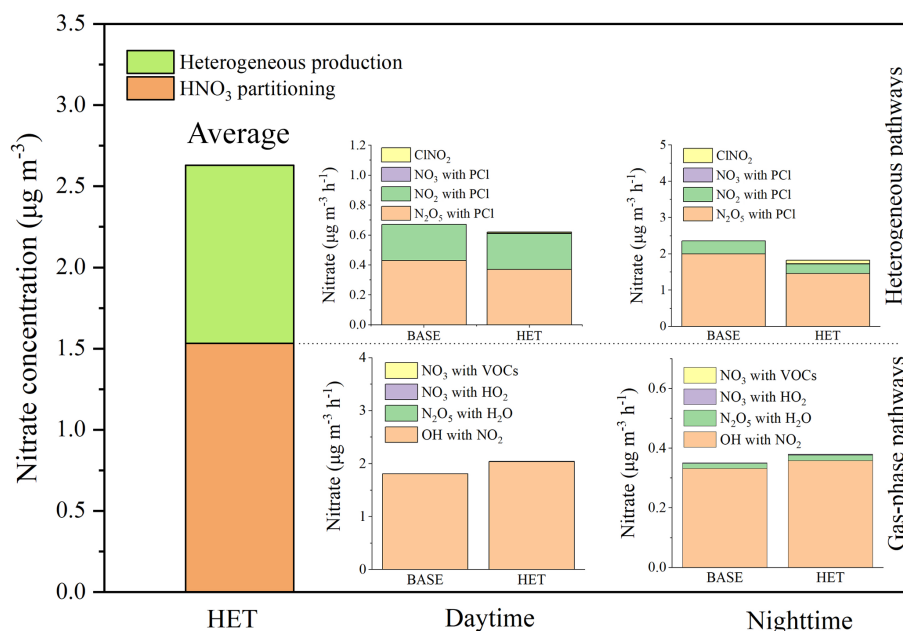


Figure 4. Contributions of different homogeneous and heterogeneous pathways to nitrate formation.

tions in the United States are significantly lower than those in Beijing (the monthly PCI concentration is $0.06 \mu\text{g m}^{-3}$ in the United States against $\sim 1 \mu\text{g m}^{-3}$ in Beijing) so that PCI is depleted quickly. The contributions of NO_2 uptake to nitrate also decrease by 22 % because of the lower rate constant of the reaction of NO_2 with PCI. In contrast, the contribution of ClNO_2 reacts with the particle surface to nitrate production increases of 6 % in the HET case. The overall nitrate concentration in the HET case is about 22 % higher than that in the BASE case during this study period.

4 Conclusions

In this work, a modified CMAQ model incorporating heterogeneous reactions for the production of molecular chlorine and other reactive chlorine species is developed, and its impact on the nitrate formation predictions is evaluated. The contributions from different homogeneous and heterogeneous pathways to nitrate formation are also quantified. High concentrations of Cl_2 and ClNO_2 do not occur in the southern part of the Beijing–Tianjin–Hebei region with intensive emissions of chlorine species, as higher concentrations of O_3 and N_2O_5 associated with the heterogeneous formation of these species generally occurred in the downwind areas. CTMs without a complete treatment of the chlorine chemistry can underestimate daytime nitrate formation from the homogeneous pathways, particularly from HNO_3 gas-to-particle partitioning due to underestimation of OH concentrations and overestimation of the nighttime nitrate formation from the heterogeneous pathways due to missing chlorine heterogeneous chemistry.

Data availability. The data in this study are available from the authors upon request (shxwang@tsinghua.edu.cn).

Supplement. The supplement related to this article is available online at: <https://doi.org/10.5194/acp-19-6737-2019-supplement>.

Author contributions. XQ, QY, SW and JH designed the study. YS, BL, AS and XY provided observation data. XQ, QY, SW, JZ, QX, DD, LD and JX analyzed data. XQ, QY and SW wrote the paper.

Competing interests. The authors declare that they have no conflict of interest.

Acknowledgements. The simulations were completed on the Explorer 100 cluster system of the Tsinghua National Laboratory for Information Science and Technology.

Financial support. This research has been supported by the National Natural Science Foundation of China (grant no. 21625701), the China Postdoctoral Science Foundation (grant no. 2018M641385), the National Research Program for Key Issue in Air Pollution Control (grant nos. DQGG0301, DQGG0501) and the National Key R&D Program of China (grant nos. 2018YFC0213805, 2018YFC0214006).

Review statement. This paper was edited by Andreas Hofzumahaus and reviewed by three anonymous referees.

References

- Abbatt, J. P. D. and Waschewsky, G. C.G.: Heterogeneous interactions of HOBr, HNO₃, O₃, and NO₂ with deliquescent NaCl aerosols at room temperature, *J. Phys. Chem. A.*, 102, 3719–3725, 1998.
- Bertram, T. H. and Thornton, J. A.: Toward a general parameterization of N₂O₅ reactivity on aqueous particles: the competing effects of particle liquid water, nitrate and chloride, *Atmos. Chem. Phys.*, 9, 8351–8363, <https://doi.org/10.5194/acp-9-8351-2009>, 2009.
- Brown, S. S. and Stutz, J.: Nighttime radical observations and chemistry, *Chem. Soc. Rev.*, 41, 6405–6447, 2012.
- Carter, W. P. and Heo, G.: Development of revised SAPRC aromatics mechanisms, *Atmos. Environ.*, 77, 404–414, 2013.
- Chang, X., Wang, S., Zhao, B., Cai, S., and Hao, J.: Assessment of inter-city transport of particulate matter in the Beijing–Tianjin–Hebei region, *Atmos. Chem. Phys.*, 18, 4843–4858, <https://doi.org/10.5194/acp-18-4843-2018>, 2018.
- Davis, J. M., Bhave, P. V., and Foley, K. M.: Parameterization of N₂O₅ reaction probabilities on the surface of particles containing ammonium, sulfate, and nitrate, *Atmos. Chem. Phys.*, 8, 5295–5311, <https://doi.org/10.5194/acp-8-5295-2008>, 2008.
- Deiber, G., George, Ch., Le Calvé, S., Schweitzer, F., and Mirabel, Ph.: Uptake study of ClONO₂ and BrONO₂ by Halide containing droplets, *Atmos. Chem. Phys.*, 4, 1291–1299, <https://doi.org/10.5194/acp-4-1291-2004>, 2004.
- Deng, S., Zhang, C., Liu, Y., Cao, Q., Xu, Y. Y., Wang, H. L., and Zhang, F.: A Full-Scale Field Study on Chlorine Emission of Pulverized Coal-Fired Power Plants in China, *Research of Environmental Science*, 27, 127–133, 2014 (in Chinese).
- Faxon, C. B., Bean, J. K., and Hildebrandt R. L.: Inland Concentrations of Cl₂ and ClNO₂ in Southeast Texas Suggest Chlorine Chemistry Significantly Contributes to Atmospheric Reactivity, *Atmosphere*, 6, 1487–1506, 2015.
- Fu, X., Wang, S. X., Chang, X., Xing, J., and Hao, J. M.: Modeling analysis of secondary inorganic aerosols over China: pollution characteristics, and meteorological and dust impacts, *Sci. Rep.*, 6, 35992, <https://doi.org/10.1038/srep35992>, 2016.
- Fu, X., Wang, T., Wang, S. X., Zhang, Lei, Cai, S. Y., Xing, J., and Hao, J. M.: Anthropogenic Emissions of Hydrogen Chloride and Fine Particulate Chloride in China, *Environ. Sci. Technol.*, 52, 1644–1654, 2018.
- Gebel, M. E. and Finlayson-Pitts, B. J.: Uptake and reaction of ClONO₂ on NaCl and synthetic sea salt, *J. Phys. Chem. A.*, 105, 5178–5187, 2001.
- George, I. J. and Abbatt, J. P.: Heterogeneous oxidation of atmospheric aerosol particles by gas-phase radicals, *Nat. Chem.* 2, 713–722, 2010.
- Glasow, V. R.: Wider role for airborne chlorine, *Nature*, 464, 168–169, 2010.
- Goodman, A. L., Underwood, G. M., and Grassian, V. H.: Heterogeneous reaction of NO₂: characterization of gas-phase and adsorbed products from the reaction, 2NO₂(g) + H₂O(a) → HONO(g) + HNO₃(a) on Hydrated Silica Particles, *J. Phys. Chem. A.*, 103, 7217–7223, 1999.
- Hu, J., Chen, J., Ying, Q., and Zhang, H.: One-year simulation of ozone and particulate matter in China using WRF/CMAQ modeling system, *Atmos. Chem. Phys.*, 16, 10333–10350, <https://doi.org/10.5194/acp-16-10333-2016>, 2016.
- Hu, J., Wang, P., Ying, Q., Zhang, H., Chen, J., Ge, X., Li, X., Jiang, J., Wang, S., Zhang, J., Zhao, Y., and Zhang, Y.: Modeling biogenic and anthropogenic secondary organic aerosol in China, *Atmos. Chem. Phys.*, 17, 77–92, <https://doi.org/10.5194/acp-17-77-2017>, 2017.
- Jobson, B. T., Niki, H., Yokouchi, Y., Bottenheim, J. W., Hopper, F., and Leitch, R. J.: Measurements of C₂–C₆ hydrocarbons during the Polar Sunrise 1992 experiment: Evidence for Cl atom and Br atom chemistry, *J. Geophys. Res.*, 99, 25355–25368, 1994.
- Keene, W. C., Pszenny, A. A. P., Jacob, D. J., Duce, R. A., Galloway, J. N., Schultz-Tokos, J. J., Sievering, H., and Boatman, J. F.: The Geochemical Cycling of Reactive Chlorine through the Marine Troposphere, *Global Biogeochem.*, 4, 407–430, 1990.
- Keene, W. C., Khalil, M. A. K., Erickson, D. J., McCulloch, A., Graedel, T. E., Lobert, J. M., Aucott, M. L., Gong, S. L., Harper, D. B., Kleiman, G., Midgley, P., Moore, R. M., Seuzaret, C., Sturges, W. T., Benkovitz, C. M., Koropalov, V., Barrie, L., and Li, Y. F.: Composite global emissions of reactive chlorine from anthropogenic and natural sources: Reactive Chlorine Emissions Inventory, *J. Geophys. Res.-Atmos.*, 104, 8429–8440, 1999.
- Kleeman, M. J., Ying, Q., and Kaduwela, A.: Control strategies for the reduction of airborne particulate nitrate in California's San Joaquin Valley, *Atmos. Environ.*, 39, 5325–5341, 2005.
- Knipping, E. M., Lakin, M. J., Foster, K. L., Jungwirth, P., Tobias, D. J., Gerber, R. B., Dabdub, D., and Finlayson-Pitts, B. J.: Experiments and simulations of ion-enhanced interfacial chemistry on aqueous NaCl aerosols, *Science*, 288, 301–306, 2000.
- Li, H., Zhang, Q., Zheng, B., Chen, C., Wu, N., Guo, H., Zhang, Y., Zheng, Y., Li, X., and He, K.: Nitrate-driven urban haze pollution during summertime over the North China Plain, *Atmos. Chem. Phys.*, 18, 5293–5306, <https://doi.org/10.5194/acp-18-5293-2018>, 2018.
- Li, Q., Zhang, L., Wang, T., Tham, Y. J., Ahmadov, R., Xue, L., Zhang, Q., and Zheng, J.: Impacts of heterogeneous uptake of dinitrogen pentoxide and chlorine activation on ozone and reactive nitrogen partitioning: improvement and application of the WRF-Chem model in southern China, *Atmos. Chem. Phys.*, 16, 14875–14890, <https://doi.org/10.5194/acp-16-14875-2016>, 2016.
- Liu, X. X., Qu, H., Huey, L. G., Wang, Y. W., Sjostedt, S., Zeng, L. M., Lu, K. D., Wu, Y. S., Hu, M., Shao, M., Zhu, T., and Zhang, Y. H.: High Levels of Daytime Molecular Chlorine and Nitryl Chloride at a Rural Site on the North China Plain, *Environ. Sci. Technol.*, 51, 9588–9595, 2017.
- Liu, Y., Fan, Q., Chen, X., Zhao, J., Ling, Z., Hong, Y., Li, W., Chen, X., Wang, M., and Wei, X.: Modeling the impact of chlorine emissions from coal combustion and prescribed waste incineration on tropospheric ozone formation in China, *Atmos. Chem. Phys.*, 18, 2709–2724, <https://doi.org/10.5194/acp-18-2709-2018>, 2018.
- Ma, X. Y., Sha, T., Wang, J. Y., Jia, H. L., and Tian, R.: Investigating impact of emission inventories on PM_{2.5} simulations over North China Plain by WRF-Chem, *Atmos. Environ.*, 195, 125–140, 2018.
- McDuffie, E. E., Fibiger, D. L., Dubé, W. P., Hilfiker, F., Lee, B. H., Thornton, J. A., Shah, V., Jaeglé, V., Guo, H. Y., Weber, R. J., Reeves, J. M., Weinheimer, A. J., Schroder, C., Campuzano-Jost, P., Jimenez, J., Dibb, J. E., Veres, P., Ebben, C., Sparks, T. L., Wooldridge, P. J., Cohen, R. C., Hornbrook, R. S., Apel, E.

- C., Campos, T., Hall, S. R., Ullmann, K., and Brown, S. S.: Heterogeneous N_2O_5 uptake during winter: Aircraft measurements during the 2015 WINTER campaign and critical evaluation of current parameterizations, *J. Geophys. Res.-Atmos.*, 123, 4345–4372, 2018a.
- McDuffie, E. E., Fibiger, D. L., Dubé, W. P., Hilfiker, F., Lee, B. H., Thornton, J. A., Shah, V., Jaeglé, V., Guo, H. Y., Weber, R. J., Reeves, J. M., Weinheimer, A. J., Schroder, C., Campuzano-Jost, P., Jimenez, J., Dibb, J. E., Veres, P., Ebben, C., Sparks, T. L., Wooldridge, P. J., Cohen, R. C., Hornbrook, R. S., Apel, E. C., Campos, T., Hall, S. R., Ullmann, K., and Brown, S. S.: ClNO_2 yields from aircraft measurements during the 2015 WINTER campaign and critical evaluation of the current parameterization, *J. Geophys. Res.-Atmos.*, 123, 12–994, 2018b.
- Osthoff, H. D., Roberts, J. M., and Ravishankara, A. R.: High levels of nitryl chloride in the polluted subtropical marine boundary layer, *Nat. Geosci.*, 1, 324–328, 2008.
- Pratte, P. and Rossi, M. J.: The heterogeneous kinetics of HOBr and HOCl on acidified sea salt and model aerosol at 40–90 % relative humidity and ambient temperature, *Phys. Chem. Chem. Phys.*, 8, 3988–4001, 2006.
- Qiu, X. H., Chai, F. H., Duan, L., Chai, F. H., Wang, S. X., Yu, Q., and Wang, S. L.: Deriving High-Resolution Emission Inventory of Open Biomass Burning in China based on Satellite Observations, *Environ. Sci. Technol.*, 50, 11779–11786, 2016.
- Riedel, T. P., Bertram, T. H., Crisp, T. A., Williams, E. J., Lerner, B. M., Vlasenko, A., Li, S. M., Gilman, J., de Gouw, J., Bon, D. M., Wagner, N. L., Brown, S. S., and Thornton, J. A.: Nitryl Chloride and Molecular Chlorine in the Coastal Marine Boundary Layer, *Environ Sci Technol.*, 46, 10463–10470, 2012.
- Roberts, J. M., Osthoff, H. D., Brown, S. S., and Ravishankara, A. R.: N_2O_5 oxidizes chloride to Cl_2 in acidic atmospheric aerosol, *Science*, 321, 1059–1059, 2008.
- Rossi, M. J.: Heterogeneous Reactions on Salts, *Chem. Rev.*, 103, 4823–4882, 2003.
- Rudich, Y., Talukdar, R. K., Ravishankara, A. R., and Fox, R. W.: Reactive uptake of NO_3 on pure water and ionic solutions, *J. Geophys. Res.*, 101, 21023–21031, 1996.
- Sarwar, G., Simon, H., Bhawe, P., and Yarwood, G.: Examining the impact of heterogeneous nitryl chloride production on air quality across the United States, *Atmos. Chem. Phys.*, 12, 6455–6473, <https://doi.org/10.5194/acp-12-6455-2012>, 2012.
- Sarwar, G., Simon, H., and Xing, J.: Importance of tropospheric ClNO_2 chemistry across the Northern Hemisphere, *Geophys. Res. Lett.*, 41, 4050–4058, 2014.
- Seinfeld, J. H. and Pandis, S. N.: Atmospheric Chemistry and Physics: From Air Pollution to Climate Change, Wiley-Interscience, New York, USA, 2006.
- Spicer, C. W., Chapman, E. G., Finlayson-Pitts, B. J., Plastridge, R. A., Hubbe, J. M., Fast, J. D., and Berkowitz, C. M.: Unexpectedly high concentrations of molecular chlorine in coastal air, *Nature*, 394, 353–356, 1998.
- Tham, Y. J., Wang, Z., Li, Q., Wang, W., Wang, X., Lu, K., Ma, N., Yan, C., Kecorius, S., Wiedensohler, A., Zhang, Y., and Wang, T.: Heterogeneous N_2O_5 uptake coefficient and production yield of ClNO_2 in polluted northern China: roles of aerosol water content and chemical composition, *Atmos. Chem. Phys.*, 18, 13155–13171, <https://doi.org/10.5194/acp-18-13155-2018>, 2018.
- Thornton, J. A., Kercher, J. P., Riedel, T. P., Wagner, N. L., Cozic, J., Holloway, J. S., Dubé, W. P., Wolfe, G. M., Quinn, P. K., Middlebrook, A. M., Alexander, B., and Brown, S. S.: A large atomic chlorine source inferred from mid-continental reactive nitrogen chemistry, *Nature*, 464, 271–274, 2010.
- Tuazon, E. C., Atkinson, R., Plum, C. N., Winer, A. M., and Pitts Jr., J. N.: The reaction of gas phase N_2O_5 with water vapor, *Geophys. Res. Lett.*, 10, 953–956, 1983.
- Wang, H. C., Lu, K. D., Chen, X. R., Guo, S., Jiang, M. Q., Li, X., Shang, D. J., Tian, Z. F., Wu, Y. S., Wu, Z. J., Zou, Q., Zheng, Y., Zeng, L. M., Zhu, T. Hu, M., and Zhang, Y. H.: High N_2O_5 concentrations observed in urban Beijing: implications of a large nitrate formation pathway, *Environ. Sci. Technol. Lett.*, 4, 416–420, 2017.
- Wang, S. X., Zhao, B., Cai, S. Y., Klimont, Z., Nielsen, C. P., Morikawa, T., Woo, J. H., Kim, Y., Fu, X., Xu, J. Y., Hao, J. M., and He, K. B.: Emission trends and mitigation options for air pollutants in East Asia, *Atmos. Chem. Phys.*, 14, 6571–6603, <https://doi.org/10.5194/acp-14-6571-2014>, 2014.
- Wen, L., Xue, L., Wang, X., Xu, C., Chen, T., Yang, L., Wang, T., Zhang, Q., and Wang, W.: Summertime fine particulate nitrate pollution in the North China Plain: increasing trends, formation mechanisms and implications for control policy, *Atmos. Chem. Phys.*, 18, 11261–11275, <https://doi.org/10.5194/acp-18-11261-2018>, 2018.
- Wu, X. W., Chen, W. W., Wang, K., Xiu, A. J., Zhang, S. C., Zhao, H. M., and Zhang, X. L.: $\text{PM}_{2.5}$ and VOCs emission inventories from cooking in Changchun city, *China Environmental Science*, 38, 2882–2889, 2018.
- Ying, Q., Li, J. Y., and Kota, S. H.: Significant Contributions of Isoprene to Summertime Secondary Organic Aerosol in Eastern United States, *Environ. Sci. Technol.*, 49, 7834–7842, 2015.
- Young, C. J., Washenfelder, R. A., Edwards, P. M., Parrish, D. D., Gilman, J. B., Kuster, W. C., Mielke, L. H., Osthoff, H. D., Tsai, C., Pikelnaya, O., Stutz, J., Veres, P. R., Roberts, J. M., Griffith, S., Dusanter, S., Stevens, P. S., Flynn, J., Grossberg, N., Lefer, B., Holloway, J. S., Peischl, J., Ryerson, T. B., Atlas, E. L., Blake, D. R., and Brown, S. S.: Chlorine as a primary radical: evaluation of methods to understand its role in initiation of oxidative cycles, *Atmos. Chem. Phys.*, 14, 3427–3440, <https://doi.org/10.5194/acp-14-3427-2014>, 2014.
- Zhang, T., Peng, L., and Li, Y. H.: Chemical characteristics of $\text{PM}_{2.5}$ emitted from cooking fumes, *Res. Environ. Sci.*, 29, 183–191, 2016 (in Chinese).
- Zhou, W., Zhao, J., Ouyang, B., Mehra, A., Xu, W., Wang, Y., Bannan, T. J., Worrall, S. D., Priestley, M., Bacak, A., Chen, Q., Xie, C., Wang, Q., Wang, J., Du, W., Zhang, Y., Ge, X., Ye, P., Lee, J. D., Fu, P., Wang, Z., Worsnop, D., Jones, R., Percival, C. J., Coe, H., and Sun, Y.: Production of N_2O_5 and ClNO_2 in summer in urban Beijing, China, *Atmos. Chem. Phys.*, 18, 11581–11597, <https://doi.org/10.5194/acp-18-11581-2018>, 2018.